Nuclear Instruments and Methods in Physics Research A 686 (2012) 100–105

Contents lists available at SciVerse ScienceDirect

Nuclear Instruments and Methods in Physics Research A

journal homepage: www.elsevier.com/locate/nima

A novel method for detecting neutrons using low density high porosity aerogel and saturated foam

Kyle A. Nelson *, James L. Neihart, Todd A. Riedel, Aaron J. Schmidt, Douglas S. McGregor

S.M.A.R.T. Laboratory, Mechanical and Nuclear Engineering, Kansas State University, Manhattan, KS 66506, USA

ARTICLE INFO

Article history:
Received 18 November 2011
Received in revised form
3 April 2012
Accepted 27 April 2012
Available online 11 May 2012

Keywords:
^{3}He replacement
Neutron detection
Aerogel
Foam

ABSTRACT

As a result of the recent shortage of ^{3}He for neutron detection, several new detectors have been proposed as viable alternatives. Thin-film coated diodes and boron-lined proportional counters are suggested options, but both suffer from the "wall-effect", where only one interaction product can be measured per event. The "wall-effect" greatly reduces the neutron detection efficiency of the device. A new method is presented using low-density high-porosity materials where both reaction products can escape the absorber and contribute to a single event. Measuring both reaction products simultaneously greatly increases the detection efficiency of the device. Experimentally obtained pulse-height spectra from saturated foam and borosilicate aerogel detectors are presented. Aerogel is a low-density solid, typically less than 50 mg/cm^{3}, and can be developed with ^{10}B in the structure. The thermal neutron response pulse-height spectrum from borosilicate aerogel is presented. Additionally, polyurethane foam, another low-density high-porosity material, was saturated with LiF and B_2O_3 to levels greater than 20 percent by weight and tested as a neutron detection medium. The foam saturated with 4.5 percent ^{6}LiF was cut into 10 sheets, each 2 mm thick, and a neutron response pulse-height spectrum was collected. The thermal neutron detection efficiency was measured to be 7.3 percent, and the neutron to gamma-ray rejection ratio, acquired using a ^{137}Cs gamma-ray source, was calculated to be 1.71×10^{6}. Theoretical calculations also show that neutron detection efficiencies above 60 percent can be easily achieved using enriched ^{6}LiF foam at 20 percent or higher saturation levels.

1. Introduction

There is a critical ^{3}He shortage and significant effort has been invested to find and/or develop a practical alternative medium for neutron detection. To replace a ^{3}He gas-filled proportional counter, the detector is required to have high neutron sensitivity, large area, and high gamma-ray discrimination. Several options have been proposed [1,2], but suffer from either low efficiency, poor gamma-ray discrimination, or high cost. A number of different materials are known to absorb neutrons readily, e.g., ^{6}Li, ^{10}B, ^{113}Cd, and ^{157}Gd, and have been used as neutron reactive materials for detection systems [3–15]. However, the focus can be narrowed to ^{6}Li and ^{10}B due to the large Q-value and short ranges of their reaction products, which are ideal for gas-filled neutron detectors. The microscopic thermal neutron (0.0259 eV) absorption cross-sections for ^{6}Li and ^{10}B are 940 b and 3840 b, with natural abundances of 7.59 and 19.9 percent, respectively. The ^{6}Li(n,t) ^{4}He and ^{10}B(n,α) ^{7}Li reactions lead to the following reaction products, with reaction Q-values of 4.78 MeV and 2.79 MeV, respectively. The ^{10}B(n,α) ^{7}Li reaction has two branches, one branch occuring 94 percent of the time and the other the remaining 6 percent.

$$^{10}\mathrm{B} + {}^{1}_{0}\mathrm{n} \rightarrow {}^{7}\mathrm{Li}(1.015\ \mathrm{MeV}) + \alpha(1.777\ \mathrm{MeV}) \qquad 6\%$$

$$^{10}\mathrm{B} + {}^{1}_{0}\mathrm{n} \rightarrow {}^{7}\mathrm{Li}(0.840\ \mathrm{MeV}) + \alpha(1.470\ \mathrm{MeV}) + \gamma(0.480\ \mathrm{MeV}) \qquad 94\%$$

and

$$^{6}\mathrm{Li} + {}^{1}_{0}\mathrm{n} \rightarrow {}^{3}\mathrm{H}(2.73\ \mathrm{MeV}) + \alpha(2.05\ \mathrm{MeV})$$

Typically, when a coated detector absorbs slow neutrons, the reaction products are emitted in opposite directions from the ^{6}Li(n,t) ^{4}He and ^{10}B(n,α) ^{7}Li reactions. Hence, only one reaction product may enter the detecting medium, be it gas, scintillator or semiconductor, and the other reaction product will not be detected. The alternative neutron detection candidates mentioned (^{113}Cd, ^{157}Gd) emit gamma-rays and low energy conversion electrons, which are difficult to discriminate between neutron-induced events, electronic noise, or background gamma-ray interactions. Thus, these materials are non-ideal for gas-filled neutron detectors.

Some proposed alternative neutron detectors are unable to measure both reaction products simultaneously, a disadvantage that greatly lowers the neutron detection efficiency [16]. For a

* Corresponding author.
E-mail address: knelson1@ksu.edu (K.A. Nelson).

0168-9002/$ - see front matter © 2012 Elsevier B.V. All rights reserved.
http://dx.doi.org/10.1016/j.nima.2012.04.084

common ^{10}B-lined gas-filled detector, one reaction product will enter the wall onto which the coating was applied. This "wall effect" causes the loss of substantial energy, and therefore, a reduced signal-to-noise ratio. Raising the LLD to increase the signal-to-noise ratio will cause a portion of the counts from neutrons to also be lost, thereby, reducing the neutron detection efficiency. Therefore, using a detector design such that both reaction products contribute to the detection signal becomes important. In order to detect both reaction products simultaneously from a solid-form neutron sensitive material, the absorber must be thinner than the summed ranges of the interaction products.

An alternative material to using an ultra-thin neutron absorber, e.g., Li foil [17], is to use a low-density high-porosity material. The low density allows the ranges of the interaction products to extend further than found with typical solid absorbers, thereby, allowing the absorber to be thicker and more structurally rigid. If the electric field is strong enough, free charges generated in the pores of the absorber will be able to escape through the voids in the neutron sensitive material, and contribute to an event. Aerogels and foams, although having different compositions, are both materials with relatively low densities and high porosities compared to typical solid absorbers, consequently allowing the ranges of the reaction products from the ^{6}Li(n,t) ^{4}He and ^{10}B(n,α) ^{7}Li reactions to travel further than a few microns, as expected for typical solids. Aerogels and foams can be manufactured into thin sheets, thus, can be acquired with thicknesses of the order or less than the ^{6}Li(n,t) ^{4}He and ^{10}B(n,α) ^{7}Li reaction product ranges.

In the present work, a single disk of borosilicate aerogel was centered between two anode wires and placed in a thermal neutron beam. The resulting neutron response pulse-height spectrum is presented. Polyurethane foam samples saturated with ^{6}LiF and B_2O_3 were cut into 2 mm thick sheets and suspended in a continuous flow proportional gas chamber. Positioning an anode wire on either side of each sheet allows the device to measure both reaction products simultaneously. By stacking several saturated foam sheets, with alternating anode wires positioned between the absorber sheets, a large area high-efficiency neutron detector can be realized, without the use of ^{3}He gas, and can be manufactured for an extremely low cost compared to current alternatives. Theoretical calculations predict the thermal neutron detection efficiency as a function of absorber thickness and number of sheets stacked together. The experimentally obtained thermal neutron detection efficiency was measured using a ^{3}He tube and compared to the theoretical values. Additionally, a ^{137}Cs gamma-ray source was used to measure and calculate a neutron to gamma-ray rejection ratio (n/γ).

2. Theoretical considerations

Shown in Fig. 1 is a conceptual arrangement of a section of the aerogel or foam multi-wire proportional counter with an inset of a single absorber sheet [18]. Because the range of the triton is longer than the thickness of the neutron absorber, the triton has a high probability of escaping the absorber. There is a low probability that neither reaction product will escape the aerogel or foam, a probability that increases with absorber thickness. Because the summed range of the interaction products is much longer than the thickness of the absorber, there is a considerable chance that the reaction products will escape both sides of the absorber, thereby, leaving more energy in the chamber than in a conventional coated proportional counter. As the reaction products travel through the gas medium, they deposit their energy and generate free electron-ion pairs. The electrons travel to the central anode wire where the device operates as a conventional proportional counter by creating a Townsend avalanche [5,6]. The positive ions travel to the cathode of the chamber and induce a current.

The theoretical calculations used to obtain the expected intrinsic thermal neutron detection efficiency for foam and aerogel detectors have been developed and are well understood [16]. The analytical approach, using a system of equations, allows for calculations of neutron detection efficiencies for thin-film coated diode devices having various neutron absorber layers and layer thicknesses [16]. Although originally developed for coated semiconductor diodes, the same equations can be used for gas-filled detectors. The equations combine the neutron absorption probability with the probability that the reaction products will escape the absorber and enter the detector gas volume.

Using the method in the literature [16], efficiency calculations were performed using an aerogel density of 0.02 g/cm^3 and a foam density of 0.01 g/cm^3 (typical densities provided by the manufacturers) and an LLD of 300 keV. The theoretical ranges of the reaction products in the aerogel and polyurethane foam obtained using SRIM are shown in Table 1 [19]. The macroscopic thermal neutron absorption cross-section of 20 percent ^{6}LiF saturated foam is 0.23 cm^{-1} at a density of 0.01 g/cm^3. The macroscopic thermal neutron absorption cross-section of elemental ^{10}B aerogel is 4.62 cm^{-1} at a density of 0.02 g/cm^3.

Shown in Figs. 2 and 3 are the results of the theoretical thermal neutron detection efficiency calculations for 1–5, 10, 15, and 20 layers of 20 percent ^{6}LiF saturated foam and elemental ^{10}B aerogel. The plots show that for any particular number of layers of neutron absorber there is an optimum layer thickness that maximizes the intrinsic thermal neutron detection efficiency.

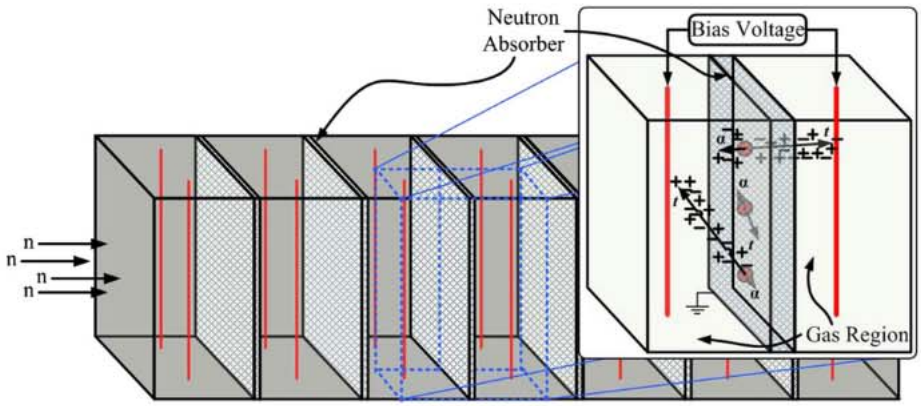

Fig. 1. A cross sectional view of the conceptual arrangement of the multi-wire proportional chamber with either saturated foam or aerogel as the neutron absorber.

Table 1
Listed are the ranges, in microns, of the reaction products from ^{10}B and ^{6}Li in elemental ^{10}B and ^{6}LiF aerogel and polyurethane foam.

	Range of the interaction products in aerogel and foam in microns					
	$^{10}B(n,\alpha)^{7}Li$				$^{6}Li(n,\alpha)^{3}H$	
	α 1.777 MeV	α 1.470 MeV	^{7}Li 1.015 MeV	^{7}Li 840 keV	^{3}H 2.73 MeV	α 2.050 MeV
Aerogel	378	285	118	93	4440	798
Foam	801	651	369	331	5580	946

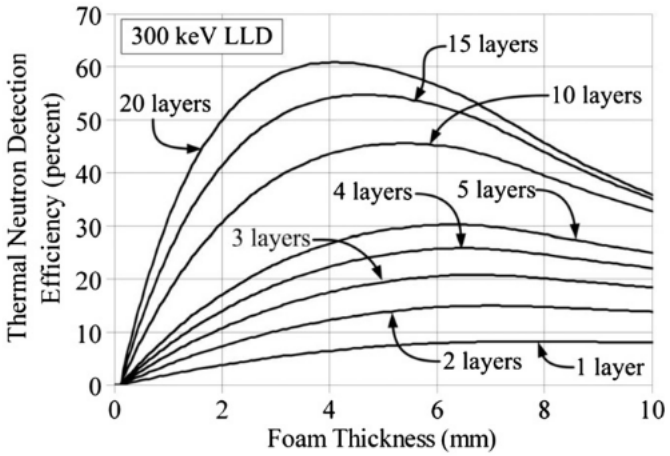

Fig. 2. Thermal neutron detection efficiency of 20% ^{6}LiF saturated foam as a function of thickness and number of layers of foam.

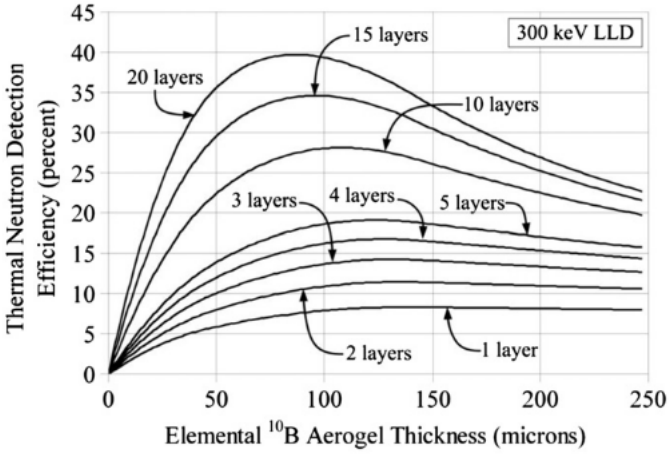

Fig. 3. Thermal neutron detection efficiency of 20 mg/cm^3 elemental ^{10}B aerogel as a function of thickness and number of layers.

The experimental neutron detection efficiency of the multi-wire proportional counter was calculated using three measurements. Measurement *a* was obtained using the multi-wire proportional counter containing the neutron absorber placed in a collimated thermalized neutron beam. Measurement *b* was collected from a ^{3}He proportional counter positioned behind the multi-wire detector, but still in the neutron beam. Measurement *c* was again collected from the ^{3}He proportional counter, but the multi-wire detector was positioned out of the neutron beam while the ^{3}He detector remained in position. The thermal neutron detection efficiency can be calculated using the following equations.

$$\left(1-\frac{b}{c}\right)=\text{Neutron Attenuation} \tag{1}$$

$$\left(\frac{a}{c\ b}\right)=\text{Neutron Fraction} \tag{2}$$

Eq. (1) is the fraction of neutrons absorbed by the multi-wire detector, or neutron attenuation of the detector. Eq. (2) is the fraction of the neutrons that are absorbed and counted by the multi-wire detector. Thus, the intrinsic thermal neutron detection efficiency is obtained by multiplying (1) and (2) together. If the ^{3}He calibration detector does not have a 100 percent thermal neutron detection efficiency, ε_{He}, the foam or aerogel detector efficiency, ε_{det}, becomes

$$\left(1-\frac{b}{c}\right)\left(\frac{a}{c\ b}\right)\varepsilon_{He}=\varepsilon_{det} \tag{3}$$

The thermal neutron detection efficiency can also be calculated using (4). However, when developing a new detector, it is helpful to know the neutron attenuation of the device. For example, a detector may absorb 90 percent of the neutrons transmitting through the detector volume, but may only have an intrinsic neutron detection efficiency of 5 percent. Eq. (1) can be used to examine the neutron attenuation of the detector, thereby, adding valuable understanding of the detector and its capabilities.

$$\left(\frac{c}{\varepsilon_{He}}\right)^{-1}=\varepsilon_{det} \tag{4}$$

3. Experimental procedure

Future Foam provided samples of polyurethane foam saturated with 4.5 percent ^{6}LiF. The ^{6}LiF saturated foam was cut into 10 sheets, each approximately 2 mm thick, and fastened in frames 15 cm × 15 cm. Ten frames, with the saturated foam, were placed in a continuous flow gas chamber 16 cm × 16 cm × 49.5 cm long, referred to as chamber *A*. Each frame was spaced 4.5 cm apart with a 25 μm thick tungsten anode wire strung centrally among spacing between each layer and the chamber walls. A thin 5 mm thick plastic chassis lining the inside of 2 of the walls in chamber *A* was used to position the frames upright. The chassis did not interfere with neutron or gamma-ray measurements.

Because the distance between foam sheets in the larger box is shorter than the range of the triton in P-10 gas (90% Ar, 10% CH_4) gas, an additional smaller chamber, 16 cm × 16 cm × 16 cm, referred to as chamber *B*, was used to obtain a better representation of the neutron response spectrum which contained only a single neutron absorber layer. The dimensions of chamber *B* are larger than the range of the triton, thus, allowing all of the energy from the triton to be absorbed in the gas volume. Although a pulse-height spectrum was obtained with chamber *A*, its main use was to obtain an intrinsic thermal neutron detection efficiency of the saturated foam using a calibrated ^{3}He tube. The chambers were placed in the 1 cm diameter collimated thermalized neutron beam at the Kansas State University (KSU) TRIGA Mark II nuclear reactor to collect pulse-height spectra and measurements, which

were performed in 600 s intervals. Prior to loading the saturated foam, pulse-height and counting curves were obtained for each chamber in order to find the ideal operating bias voltages, which were 300 V for chamber *A* and 350 V for chamber *B*. An identical experiment was performed using 20 percent B_2O_3 saturated foam as a replacement of the LiF saturated foam sheets.

To obtain the neutron detection efficiency of the ^{6}LiF saturated foam samples in chamber *A*, a 600 s pulse-height spectrum was collected at a reactor power of 1 kW. Channel number 45, found to be slightly above system noise, was used as the LLD for calculating the thermal neutron detection efficiency and the recorded counts above channel number 45 were summed, *i.e.*, measurement *a*. The ^{3}He tube was placed behind chamber *A* and another 600 s measurement was collected from the ^{3}He tube, measurement *b*, to calculate the thermal neutron attenuation of the multi-wire foam detector. An additional 600 s measurement was collected using the ^{3}He tube with chamber *A* removed from the neutron beam, measurement *c*. The intrinsic neutron detection efficiency of the 10 layers of ^{6}LiF saturated foam was calculated from the above three measurements using Eqs. (1)–(3) and subsequently compared to theoretical calculations. Chamber *B* was placed in the neutron beam, with the nuclear reactor power at 300 kW, for 30 min and a pulse-height spectrum was collected.

An additional experiment was performed to investigate the gamma-ray sensitivity using chamber *A* with 10 layers of saturated foam. A 71.6 mCi ^{137}Cs gamma-ray source was placed directly in front of the 15 cm × 15 cm face such that gamma-rays were emitted perpendicular to the face of the chamber, and an n/γ rejection ratio was calculated.

An aluminum platform was fabricated to position the borosilicate aerogel sample, provided by Aerogel Technologies, LLC, centered between two anode wires. The borosilicate aerogel sample was 2 cm in diameter and 4 mm thick. The platform was designed such that the flat faces of the aerogel sample would each be facing an anode wire, an anode wire on each side of the sample. The modified chamber *B* was placed in the 1 cm diameter diffracted thermal neutron beam and the neutron response was recorded for 30 min at 500 kW of reactor power. The borosilicate sample was replaced with a standard silica aerogel sample and the same neutron irradiation experiment was repeated. The pulse-height spectra collected from both borosilicate and silica aerogel samples were recorded and compared.

4. Experimental results

The neutron response pulse-height spectrum from 1 sheet of 10 percent natural LiF foam, chamber *B*, is shown in Fig. 4. The neutron response pulse-height spectrum of the 10 sheets of 4.5 percent ^{6}LiF foam, chamber *A*, is shown in Fig. 5 and compared to the detector spectrum that had 5 sheets at the same saturation level. Also shown in Fig. 5 is the ^{137}Cs gamma-ray response pulse-height spectrum. The intrinsic thermal neutron detection efficiency of the 10 layers of 4.5 percent ^{6}LiF saturated foam was approximately 7.3 percent using channel number 45 for the LLD and Eqs. (1)–(3). When a ^{148}Gd alpha particle source, emitting 3.18 MeV alpha particles, was placed in the multi-wire detector, the full energy peak fell in channel number 300. The energy calibration indicated that channel number 45 corresponded to 954 keV. There is a large valley between the main peak of the spectra in Figs. 4 and 5 and the electronic noise. The ratio of the minimum counts in the valley to the maximum counts in the peak is larger for the spectrum obtained from chamber *B* compared to the spectra collected from chamber *A*. A similar case is observed with the valley when 5 of the 10 frames of ^{6}LiF saturated foam from chamber *A* were removed to increase the distance between the foam sheets. The gamma-ray detection efficiency was

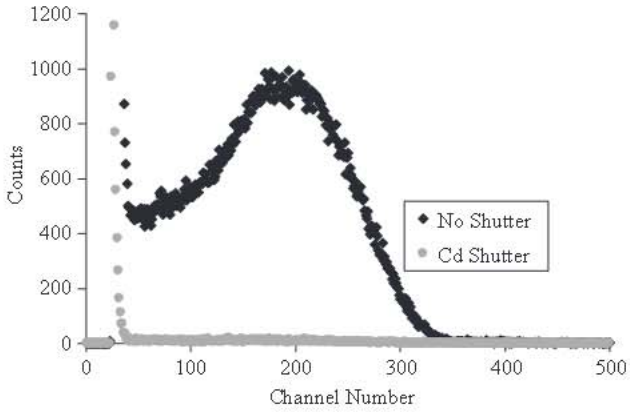

Fig. 4. The neutron response spectrum of a single foam sheet 2 mm thick with 10 percent LiF saturation.

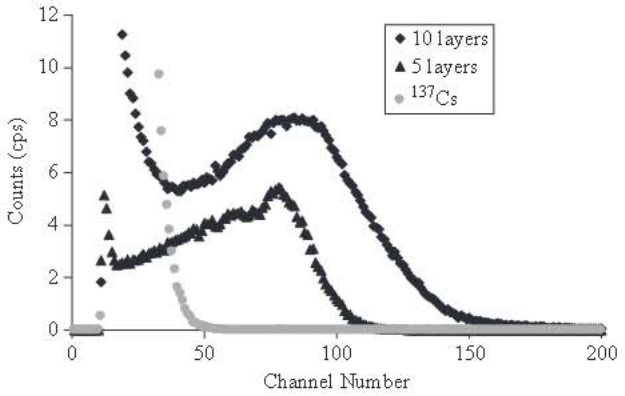

Fig. 5. The neutron response spectrum of 10 and 5 layers of 4.5 percent ^{6}LiF saturated foam. The response to the ^{137}Cs gamma ray source is also shown.

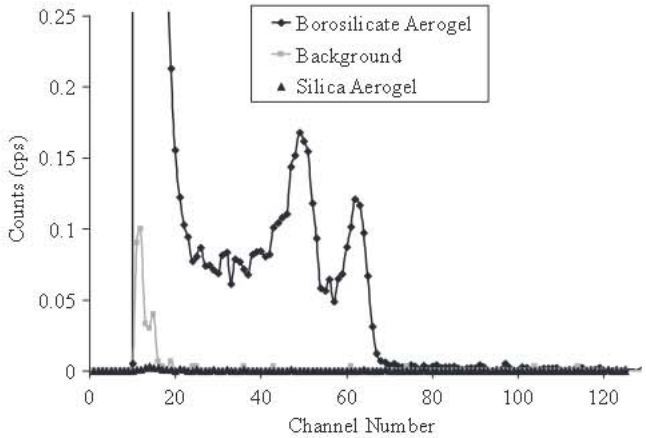

Fig. 6. The neutron response spectrum of a 4 mm thick borosilicate aerogel sample.

measured using 10 sheets and used to find the n/γ ratio. Using channel number 45 as the LLD setting, the n/γ rejection ratio was 1.71×10^6.

The neutron response pulse-height spectrum from the borosilicate aerogel is shown in Fig. 6. There are two distinct energy peaks, most likely occurring from the two reaction products. Again, similar to the LiF saturated foam spectra, there is a valley between the electronic noise and the two energy peaks. Afterwards, the borosilicate sample was replaced with a standard silica aerogel sample to ensure the response was due to neutrons and

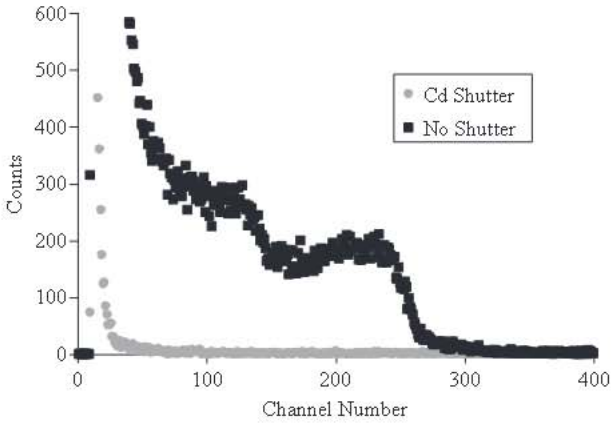

Fig. 7. The neutron response pulse-height spectrum of a single sheet of 2 mm thick 20 percent B_2O_3 saturated foam collected for 30 min.

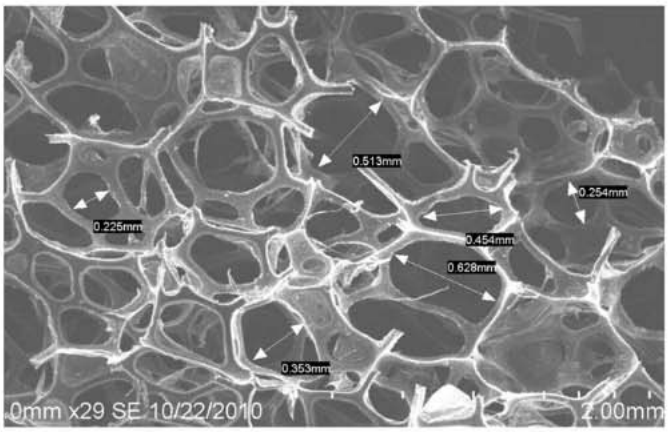

Fig. 8. Scanning electron microscope image of LiF saturated open-cell polyurethane foam.

not some unidentified interaction. Because aluminum has a negligible thermal neutron interaction cross-section, it was selected as a support structure to position the aerogel samples in the chamber. The neutron response pulse-height spectrum with the 20 percent saturated B_2O_3 foam is shown in Fig. 7. There is a distinct wall effect that is present similar to that observed with ^{10}B-lined counters. The thermal neutron detection efficiency was not calculated nor an n/γ ratio determined because there was no valley between the main features of the spectrum and the electronic noise.

5. Discussion

The pulse-height spectra from the LiF saturated foam and borosilicate aerogel proportional detectors have large valleys between the electronic noise and the main features of the neutron response spectrum, which is excellent for gamma-ray discrimination as shown by the n/γ rejection ratio. The measured n/γ rejection ratio is higher than that of ^{3}He proportional counters (typically 1×10^5) [20]. The pulse-height spectra acquired using chamber *B*, the smaller chamber, shown in Fig. 4, resembles the expected result from a prototype pressurized chamber with saturated foam. This same expected spectrum is also shown in Fig. 5, when half of the sheets are removed; the distance between each foam sheet was approximately 9 cm. The range of the 2.73 MeV triton in P-10 gas is 7.26 cm. Thus, all of the energy from the triton can be deposited in the gas region without colliding into any structures inside the chamber.

The theoretical thermal neutron detection efficiency calculated for 10 layers of 4.5 percent ^{6}LiF saturated foam is 8.5 percent. Some discrepancies in the experiment could come from error in measuring the thickness of the foam and uncertainties with the exact density of the material. The density was estimated by the saturation level, and should render a value in the correct order of magnitude. However, a difference of slightly more than one percent in the measured and theoretical thermal neutron detection efficiency is a good indicator for neutron detection efficiency expected by higher saturation levels. The source of the largest discrepancy is the range of the interaction products in foam and aerogel. The ranges were calculated in SRIM for a uniform solid [19]. However, the material is not a uniform solid but instead a porous and low-density material. The average strut size in the foam is approximately 40 μm and the average cell size is approximately 0.5 mm in diameter, as shown in the SEM image in Fig. 8. The strut size of the aerogel is on the nanometer scale along with the cell dimensions. If the theoretical ranges of the interaction products from SRIM are on the micron scale for the aerogel sample, but both reaction products can be observed in the spectrum from absorbers millimeters in thickness, then, obviously, the range of the interaction product ranges are longer than the theoretical ranges calculated from SRIM. Therefore, the theoretical calculations of the thermal neutron detection efficiency for the elemental ^{10}B aerogel and saturated foam are underestimations. Extensive research must to be performed to study and understand the interactions of charged particles in low-density high-porosity materials in order to both obtain a better estimation of the ranges of the neutron absorption reaction products and neutron sensitivity for foam and aerogel.

The ranges of the interaction products from the ^{10}B reaction are too short to escape the 2 mm thick samples of foam. Therefore, the wall effect dominates the neutron response pulse-height spectrum for B_2O_3 saturated foam samples. Cutting foam samples less than 2 mm thick becomes difficult, but the cell size and density of the foam are controllable. Increasing the cell size and decreasing the foam density will increase the probability that reaction products escape a foam sheet 2 mm thick.

Potentially, the foam samples can be fabricated in large sections. The typical foam manufacturing machine produces 6 ft × 4 ft × 100 ft slabs of foam. The foam can be cut into 2–4 mm thick sheets, 6 ft × 4 ft, and placed in a large multi-wire proportional counter. Theoretical calculations show that 10 layers of 20 percent saturated ^{6}LiF foam can achieve 40 percent or higher intrinsic thermal neutron detection efficiency. Even though the neutron detection efficiency is half that of ^{3}He proportional counters, the area is much greater, and the neutron sensitivity would be orders of magnitude higher. It would take more than 22 ^{3}He tubes, 5 cm in diameter and 2 m long, to cover the same effective area as the foam detector. Additionally, fabricating the impregnated foam is inexpensive and easy, and machines to fabricate and cut the saturated foam already exist. A single detector, similar to the one previously described in this work but 6 ft × 4 ft in cross-sectional area, would cost less than $500 for the foam neutron absorber.

The neutron detection efficiency and n/γ ratio of the borosilicate aerogel was not calculated. The amount of ^{10}B in the aerogel sample is less than 0.1 percent. Thus, calculating neutron detection efficiency would have little meaning. However, future research is aimed at increasing the ^{10}B content in the aerogel, eventually reaching that of elemental ^{10}B aerogel. Because aerogel has a similar density as the saturated foam, it is expected to have a similar n/γ rejection ratio.

6. Conclusions

The shortage of ^{3}He gas for large area neutron detectors promoted an increase in research for a viable alternative. Shown in the present

work is the potential for ^{6}LiF saturated foam and boron aerogels to replace ^{3}He neutron detectors. Although the efficiency is not as high per unit area when compared to ^{3}He, the effective area of a single detector is much larger, thereby, making the device effective at detecting neutron-emitting nuclear materials from a distance. Future work consists of increasing the saturation level of the foam and increasing the boron content in aerogels, eventually producing an elemental ^{10}B aerogel. Additionally, many form factors and designs using these materials will be explored.

Acknowledgments

This work is supported by the U.S. Defense Threat Reduction Agency (DTRA), under contract HDTRA1–12-C-0004. A special thanks for Lynn Knudson at Future Foam for fabricating the saturated foam samples. A special thanks to Aerogel Technologies, LLC for providing the borosilicate and silica aerogel samples. The authors express their gratitude to the KSU TRIGA Mark II nuclear reactor staff for their helpful assistance.

References

[1] R.T. Kouzes, J.H. Ely, PNNL-19360, April 28, 2010.
[2] R.T. Kouzes, PNNL-18388, April, 2009.
[3] W. Price, Nuclear Radiation Detection, 2nd Edition, McGraw-Hill, New York, 1964.
[4] P. Convert, J.B. Forsyth, Position-Sensitive Detection of Thermal Neutrons, Academic Press, New York, 1983.
[5] N. Tsoulfanidis, S. Landsberger, Measurement and Detection of Radiation, 3rd Edition, Taylor and Francis, New York, 2011.
[6] G.F. Knoll, Radiation Detection and Measurement, 4th Edition, Wiley, New York, 2000.
[7] B. Feigl, H. Rauch, Nuclear Instruments and Methods in Physics Research Section A 61 (1968) 349.
[8] T. Aoyama, Y. Oka, K. Honda, C. Mori, Nuclear Instruments and Methods in Physics Research Section A 314 (1992) 590.
[9] A. Mireshghi, G. Cho, J. Drewery, T. Jing, S.N. Kaplan, V. Perez-Mendez, D. Wildermuth, IEEE Transactions on Nuclear Science NS-39 (1992) 635.
[10] A. Mireshghi, G. Cho, J.S. Drewery, W.S. Hong, T. Jing, H. Lee, S.N. Kaplan, V. Perez-Mendez, IEEE Transactions on Nuclear Science NS-41 (1994) 915.
[11] F. Foulon, P. Bergonzo, A. Brambilla, C. Jany, B. Guizard, R.D. Marshall, Proceedings of Materials Research Society 487 (1998) 591.
[12] A.G. Vradii, M.I. Krapivin, L.V. Maslova, O.A. Matveev, A.Kh. Khusainov, V.K. Shashurin, Soviet Atomic Energy 42 (1977) 633.
[13] D.S. McGregor, J.T. Lindsay, R.W. Olsen, Nuclear Instruments and Methods in Physics Research Section A 381 (1996) 498.
[14] M.A. Lone, R.A. Levitt, D.A. Harrison, Atomic Data and Nuclear Data Tables 26 (1981) 511.
[15] J.K. Tuli, Thermal-Neutron-Capture Gamma Rays, BNLNCS-51647 Report, UC-34-C, Brookhaven National Laboratory, Upton, 1983.
[16] D.S. McGregor, M.D. Hammig, Y.-H. Yang, H.K. Gersch, R.T. Klann, Nuclear Instruments and Methods in Physics Research Section A 500 (2003) 272.
[17] K.A. Nelson, S.L. Bellinger, B.W. Montag, J.L. Neihart, T.A. Riedel, A.J. Schmidt, D.S. McGregor, Nuclear Instruments and Methods in Physics Research Section A 669 (2012) 79–84.
[18] S.L. Bellinger, W.J. McNeil, K.A. Nelson, M.F. Ohmes, D.S. McGregor, Gas-filled Neutron Detector Having Improved Detection Efficiency, patent pending, 2010.
[19] J. Ziegler, J. Biersack, Stopping Ranges of Ions in Matter (SRIM), version 2008.
[20] D. Reilly, N. Ensslin, H. Smit Jr., S. Kreiner (Eds.), PANDA, U.S. Government Printing Office, Washington, D.C.,1991, p. 380. ISBN 0-16-032724-5.